

See discussions, stats, and author profiles for this publication at: <https://www.researchgate.net/publication/229811689>

# LITochlebite, $\text{Ag}_2\text{PbBi}_4\text{Se}_8$ , A NEW SELENIDE MINERAL SPECIES FROM ZÁLESÍ, CZECH REPUBLIC: DESCRIPTION AND CRYSTAL STRUCTURE

Article in *The Canadian Mineralogist* · January 2011

CITATIONS

8

READS

129

6 authors, including:



**Jiří Sejkora**

National Museum, Prague, Czech Republic

304 PUBLICATIONS 1,795 CITATIONS

[SEE PROFILE](#)



**Emil Makovicky**

University of Copenhagen

106 PUBLICATIONS 1,599 CITATIONS

[SEE PROFILE](#)



**Dan Topa**

Naturhistorisches Museum Wien

175 PUBLICATIONS 1,480 CITATIONS

[SEE PROFILE](#)



**Hubert Putz**

University of Salzburg

26 PUBLICATIONS 210 CITATIONS

[SEE PROFILE](#)

Some of the authors of this publication are also working on these related projects:



New minerals from Slovakia [View project](#)



Carbon minerals [View project](#)

## LITOCHELBITE, $\text{Ag}_2\text{PbBi}_4\text{Se}_8$ , A NEW SELENIDE MINERAL SPECIES FROM ZÁLESÍ, CZECH REPUBLIC: DESCRIPTION AND CRYSTAL STRUCTURE

JIRÍ SEJKORA

*Department of Mineralogy and Petrology, National Museum, Václavské náměstí 68, CZ-115 79 Praha 1, Czech Republic*

EMIL MAKOVICKY

*Department of Geography and Geology, University of Copenhagen, Østervoldgade 10, DK-1350 Copenhagen, Denmark*

DAN TOPA, HUBERT PUTZ AND GEORG ZAGLER

*Department of Materials Research and Physics, Paris-Lodron University of Salzburg, Hellbrunnerstr. 34, A-5020 Salzburg, Austria*

JAKUB PLÁŠIL

*Department of Geological Sciences, Faculty of Science, Masaryk University, Kotlářská 2, CZ-602 00 Brno, Czech Republic*

### ABSTRACT

Litochlebite,  $\text{Ag}_2\text{PbBi}_4\text{Se}_8$ , is a new selenide mineral from the Zálesí uranium deposit, Rychlebské hory Mountains, northern Moravia, Czech Republic. It occurs as irregular grains up to 200  $\mu\text{m}$ , which form aggregates up to 1–2 mm in size in a quartz gangue. These aggregates are replaced along the margins and fractures by a heterogeneous supergene Bi–Se–O phase. Other associated minerals included uraninite, hematite, and uranophane. Litochlebite is opaque, dark grey to black, has a dark grey streak and a metallic luster. No cleavage was observed; the mineral is brittle with an irregular fracture. The  $\text{VHN}_{10g}$  microhardness 230 (227–234)  $\text{kg/mm}^2$  corresponds to a Mohs hardness of about 3; the calculated density is 7.90  $\text{g/cm}^3$ . In reflected light, litochlebite is white, with weak bireflectance (only in oil) and pleochroism from white with a very faint yellowish tint to white with a very faint bluish tint. Between crossed polars, the anisotropy is moderate both in air and in oil, with dark grey to brown polarization-colors. Reflectance values in air ( $R_{\min}$ ,  $R_{\max}$  in %,  $\lambda$  nm) are: 44.5–49.9 (470), 45.1–50.5 (546), 45.6–51.3 (589), 45.4–51.8 (650). Litochlebite is monoclinic, space group  $P2_1/m$ , with  $a$  13.182(2),  $b$  4.1840(8),  $c$  15.299(2) Å,  $\beta$  109.11(1)°,  $V$  797.3(2) Å<sup>3</sup>, and  $a:b:c$  3.1506:1:3.6565. The main lines of the X-ray powder-diffraction pattern [ $d$  in Å( $hkl$ )] are: 3.684(53) (301), 3.201(76)(104), 3.028(100)(31 $\bar{1}$ ), 2.980(88)(31 $\bar{2}$ ) and 2.892(95)(005). Its average composition (electron-microprobe data) is Cu 0.10, Ag 10.27, Cd 0.05, Pb 11.73, Bi 43.27, Se 32.93, S 0.01, total 98.36 wt.%. The resulting empirical formula, written on the basis 15 *apfu*, is  $(\text{Ag}_{1.84}\text{Cu}_{0.03})_{\Sigma 1.87}(\text{Pb}_{1.09}\text{Cd}_{0.01})_{\Sigma 1.10}\text{Bi}_{3.99}\text{Se}_{8.04}$ . The ideal formula,  $\text{Ag}_2\text{PbBi}_4\text{Se}_8$ , requires Ag 11.41, Pb 10.96, Bi 44.22, Se 33.41, total 100.00 wt.%. The crystal structure of litochlebite has been solved by direct methods and refined to  $R_1 = 3.89\%$  on the basis of 938 unique reflections [ $F_o > 4\sigma(F_o)$ ] collected on a Bruker AXS diffractometer with a CCD detector and  $\text{MoK}\alpha$  radiation. The crystal structure contains one lead site, four independent Bi sites, four silver sites and eight independent Se sites. One Ag site is an octahedrally coordinated (2 + 4) site in the pseudotetragonal layer, the other Ag site has a distorted tetrahedral coordination. The remaining Ag sites have low occupancies. Litochlebite is an Ag-dominant isotype of watkinsonite,  $\text{Cu}_2\text{PbBi}_4\text{Se}_8$ , and structurally related to berryite,  $\text{Cu}_3\text{Ag}_2\text{Pb}_3\text{Bi}_7\text{S}_{16}$ .

**Keywords:** litochlebite, new mineral species, selenide, crystal structure, Zálesí uranium deposit, Czech Republic.

### SOMMAIRE

La litochlebite,  $\text{Ag}_2\text{PbBi}_4\text{Se}_8$ , est une nouvelle espèce de sélénure découverte à Zálesí, gisement d'uranium situé dans les montagnes Rychlebské hory du nord de la Moravie, en République Tchèque. Elle se présente en grains irréguliers atteignant 200  $\mu\text{m}$  en agrégats de 1 à 2 mm englobés dans le quartz. Ces agrégats sont remplacés le long des bordures et des fractures par une phase hétérogène supergène contenant Bi–Se–O. Lui sont associés uraninite, hématite, et uranophane. La litochlebite est opaque,

§ E-mail address: jiri\_sejkora@nm.cz

gris foncé ou noire, avec une rayure gris foncé et un éclat métallique. Aucun clivage n'est évident; le minéral est cassant, avec une fracture irrégulière. La microdureté  $VHN_{10g}$  de 230 (227–234)  $kg/mm^2$  correspond à une dureté de Mohs d'environ 3; la densité calculée est égale à 7.90  $g/cm^3$ . En lumière réfléchie, la lithochlebite paraît blanche, avec faible biréflectance (seulement dans l'huile) et pléochroïsme allant de blanc avec une teinte jaunâtre très légère au blanc avec une teinte bleuâtre très légère. Entre nicols croisés, l'anisotropie est modérée dans l'air ainsi que dans l'huile, avec couleurs de polarisation gris foncé à brun. Les valeurs de réflectance dans l'air ( $R_{min}$ ,  $R_{max}$  in %,  $\lambda$  nm) sont: 44.5–49.9 (470), 45.1–50.5 (546), 45.6–51.3 (589), 45.4–51.8 (650). La lithochlebite est monoclinique, groupe spatial  $P2_1/m$ , avec  $a$  13.182(2),  $b$  4.1840(8),  $c$  15.299(2) Å,  $\beta$  109.11(1)°,  $V$  797.3(2) Å<sup>3</sup>, et  $a:b:c$  3.1506:1:3.6565. Les raies principales du spectre de diffraction, méthode des poudres [ $d$  en Å( $hkl$ )] sont: 3.684(53)(301), 3.201(76)(104), 3.028(100)(311), 2.980(88)(312) et 2.892(95)(005). La composition moyenne, établie avec une microsonde électronique, est Cu 0.10, Ag 10.27, Cd 0.05, Pb 11.73, Bi 43.27, Se 32.93, S 0.01, pour un total de 98.36% (poids). La formule empirique qui en résulte, sur une base de 15 *apfu*, est  $(Ag_{1.84}Cu_{0.03})_{\Sigma 1.87}(Pb_{1.09}Cd_{0.01})_{\Sigma 1.10}Bi_{3.99}Se_{8.04}$ . La formule idéale,  $Ag_2PbBi_4Se_8$ , requiert Ag 11.41, Pb 10.96, Bi 44.22, Se 33.41, total 100.00%. Nous avons résolu la structure de la lithochlebite par méthodes directes et nous l'avons affiné jusqu'à un résidu  $R_1$  de 3.89% en nous servant de 938 réflexions uniques [ $F_o > 4\sigma(F_o)$ ] prélevées avec un diffractomètre Bruker AXS muni d'un détecteur CCD avec rayonnement  $MoK\alpha$ . La structure contient un site pour le Pb, quatre sites indépendants de Bi, quatre sites Ag et huit sites Se indépendants. Un site Ag possède une coordination octaédrique (2 + 4) dans une couche pseudotétraogonale, et un autre site Ag possède une coordination tétraédrique difforme. Les autres sites Ag ne sont que faiblement occupés. La lithochlebite est un isotype à dominance de Ag de la watkinsonite,  $Cu_2PbBi_4Se_8$ , apparentée structurellement à la berryite,  $Cu_3Ag_2Pb_3Bi_7S_{16}$ .

(Traduit par la Rédaction)

**Mots-clés:** lithochlebite, nouvelle espèce minérale, séléniure, structure cristalline, gisement uranifère de Zálesí, République Tchèque.

## INTRODUCTION

Lithochlebite, the Ag analogue of watkinsonite, was found among other selenide minerals at the abandoned Zálesí uranium deposit, Czech Republic, during an extensive program of research focused on its primary and supergene mineralization (Sejkora *et al.* 2004, 2006, 2008, in prep., Frost *et al.* 2009, 2010a, 2010b, Topa *et al.* 2010a). Zálesí is also the type locality of the Ca–Cu arsenate *zálesítite* (Sejkora *et al.* 1999).

The name *lithochlebite* honors the Czech mineralogist Dr. Jiří Litochleb (b. 1948), currently head of the Department of Mineralogy and Petrology and director of the Natural History Museum, National Museum, Praha, Czech Republic. Dr. Litochleb is the author of numerous papers on uranium, base metal, and gold ore deposits and on the mineralogy of Bi sulfo-seleno-tellurides, selenides, and sulfosalts from the Czech Republic. The mineral data and name have been approved by the IMA Commission on New Minerals and Mineral Names (IMA 2009–036). Pronunciation of the name can be transcribed as *littokhlebite*, with the 'ch' group having the same phonetic value as in Scottish (*e.g.*, *loch*) and *e* pronounced as in *get*. The holotype specimen of lithochlebite has been deposited in the mineral collection of the National Museum, Prague, Czech Republic (catalogue number PIP 11/2009).

## OCCURRENCE

Two hand samples with lithochlebite were found in mine dump material that originated from unnamed exploratory shafts in the area of the outcrops of the

Pavel vein-structure at the small Zálesí uranium deposit. This deposit is situated at the southern margin of the Zálesí settlement, about 6.5 km southwest of Javorník, Rychlebské hory Mountains, northern Moravia, Czech Republic.

The Zálesí deposit was discovered during a regional program of uranium exploration; it was exploited in a shallow shaft named Pavel and mined from Galleries I – III at five levels at vertical intervals of 50 m. Over 400 t of uranium were extracted there during 11 years of exploitation (1958–1968). Thirty hydrothermal veins and two stockworks are hosted by a folded and metamorphosed Paleozoic sequence of the Strónia Group, belonging to the Orlice–Sniežnik crystalline complex (Fojt *et al.* 2005, Sejkora *et al.* 2006). The primary mineralization of the deposit was formed in three main stages: the uraninite, arsenide, and sulfide stage, respectively, and may be classified as a representative of the so-called “five-elements” formation (U–Ni–Co–As–Ag) (Fojt *et al.* 2005, Dolníček *et al.* 2009). The relatively abundant selenide mineralization is associated with the oldest, uraninite stage of mineralization (Fojt *et al.* 2005, Sejkora *et al.* 2006). Clausthalite and naumanite are the most abundant selenides; bohdanowiczite, unnamed  $Bi_4Se_3$  (Fojt *et al.* 2005, Sejkora *et al.* 2006), watkinsonite, and S-rich umangite (Topa *et al.* 2010a, Sejkora *et al.*, in prep.) are less abundant. The Bi selenides of the ikonolite–laitakarite series were formed only sporadically at the arsenide stage (Fojt *et al.* 2005).

At Zálesí, lithochlebite formed as a primary mineral at the uraninite stage of mineralization, associated with primary quartz, uraninite, hematite and supergene uranophane and a heterogeneous Bi–Se–O phase.

## PHYSICAL PROPERTIES

Litochlebite occurs as irregular grains up to 200  $\mu\text{m}$ , forming aggregates up to 1–2 mm in size in a quartz gangue. Aggregates of this mineral are replaced along margins and fractures by the heterogeneous supergene Bi–Se–O phase (Fig. 1). Litochlebite aggregates are opaque, dark grey to black, and have a dark grey streak and a metallic luster. It does not fluoresce under both short- and long-wave ultraviolet light. No cleavage was observed; it is brittle with an irregular fracture. The  $\text{VHN}_{10g}$  microhardness, equal to 230 (227–234)  $\text{kg}/\text{mm}^2$  (three indentations), corresponds to a Mohs hardness of

about 3. Its density could not be measured owing to the small grain-size; the calculated density,  $7.90 \text{ g}/\text{cm}^3$ , is based on the empirical formula and unit-cell parameters refined from X-ray powder data.

In reflected light, litochlebite is white, with a weak bireflectance (only in oil) and a pleochroism from white with a very faint yellowish tint (darkest position) to white with a very faint bluish tint (lightest position). Internal reflections and twinning were not observed. Between crossed polars, the anisotropy is moderate both in air and in oil, with dark grey to brown polarization-colors. Reflectance data in air measured on a random section are given in Table 1. The reflectance curves of litochlebite are compared in Figure 2 with those of watkinsonite from the Otish Mountains (Johan *et al.* 1987). The  $R_{\text{min}}$  values for both minerals are very close; more significant differences (1.5–3%) are observed for  $R_{\text{max}}$  values.

TABLE 1. REFLECTANCE DATA IN AIR FOR LITOCHELBITE

$\lambda$ (nm)	$R_{\text{min}}$	$R_{\text{max}}$	$\lambda$ (nm)	$R_{\text{min}}$	$R_{\text{max}}$
400	41.5	48.9	560	45.2	50.9
420	43.0	49.1	580	45.6	51.2
440	44.4	49.7	<b>589</b>	<b>45.6</b>	<b>51.3</b>
460	44.1	49.3	600	45.4	51.4
<b>470</b>	<b>44.5</b>	<b>49.9</b>	620	45.4	51.7
480	44.8	50.2	640	45.1	51.7
500	45.1	49.9	<b>650</b>	<b>45.4</b>	<b>51.8</b>
520	44.8	50.1	660	45.4	51.9
540	44.9	50.4	680	45.2	51.6
<b>546</b>	<b>45.1</b>	<b>50.5</b>	700	44.9	51.8

Leitz MPV-SP microscope-spectrophotometer, standard: WTIC. Shown in bold are measurements at the COM wavelengths.

## CHEMICAL COMPOSITION

Quantitative chemical data for the litochlebite samples were obtained on two different electron-microprobe instruments. Initially, at the Laboratory of Electron Microscopy and Microanalysis of Masaryk University and Czech Geological Survey, Brno, litochlebite (19 analyses on four grains) were analyzed with a Cameca SX-100 electron microprobe in the wavelength-dispersion mode with an accelerating

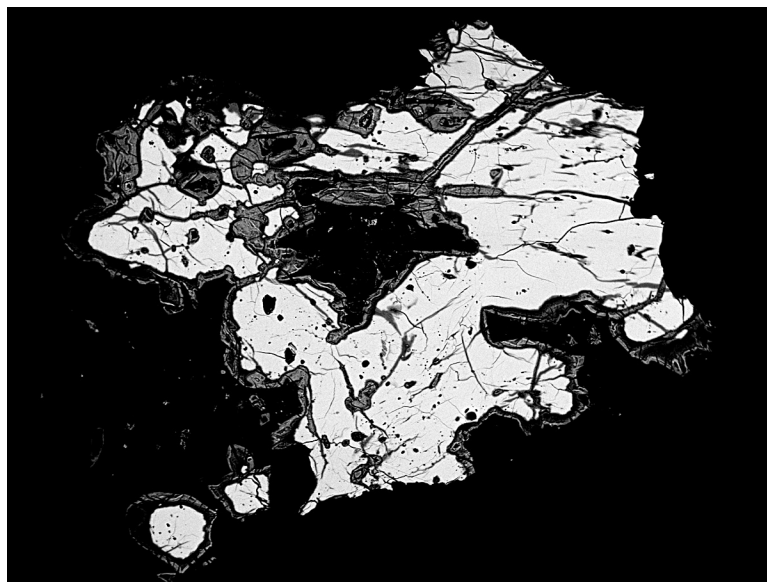


FIG. 1. BSE photograph of an irregular aggregate of litochlebite (white), partly replaced along margins and fractures by a heterogeneous Bi–Se–O phase (dark grey). Zálesí, Czech Republic; width of the field of view is 0.8 mm.

voltage of 25 kV, a specimen current of 20 nA, and a beam diameter of about 1  $\mu\text{m}$ . The following standards and X-ray lines were used: Cu ( $\text{CuK}\alpha$ ), Ag ( $\text{AgL}\alpha$ ), PbSe ( $\text{SeL}\beta$ ),  $\text{CuFeS}_2$  ( $\text{SK}\alpha$ ), CdTe ( $\text{CdL}\beta$ ), PbS ( $\text{PbM}\alpha$ ), Sb ( $\text{SbL}\beta$ ) and Bi ( $\text{BiM}\beta$ ). Peak counting times (CT) were 20 s for all elements, and CT for each background was one half of the peak time. Raw intensities were converted to concentrations using automatic PAP (Pouchou & Pichoir 1985) matrix-correction software.

Later, a JEOL Superprobe JXA-8600 apparatus (Department of Geography and Geology, University of Salzburg) operated in WDS mode was used, at 25 kV and 30 nA, with a defocused beam ( $\sim 3 \mu\text{m}$ ); measurement time was 15 s for peak and 5 s for background counts (14 analyses on two grains used for the single-crystal study). The following standards and X-ray lines were used: natural  $\text{CuFeS}_2$  (chalcopyrite;  $\text{CuK}\alpha$ ), natural PbS (galena  $\text{PbL}\alpha$ ), synthetic  $\text{Bi}_2\text{Se}_3$  ( $\text{BiL}\alpha$ ,  $\text{SeL}\alpha$ ), synthetic  $\text{Bi}_2\text{S}_3$  ( $\text{SK}\alpha$ ), synthetic CdTe ( $\text{CdL}\alpha$ ) and Ag metal ( $\text{AgL}\alpha$ ). The raw data were corrected with the on-line ZAF-4 procedure.

Analytical results obtained from the two electron microprobes (Table 2) are similar and correspond very well with the formula  $\text{Ag}_2\text{PbBi}_4\text{Se}_8$  derived from the crystal-structure study. At the Ag sites of lithochlebite, variable Cu contents (up to 0.14 *apfu*) were determined. The existence at least limited  $\text{AgCu}_{-1}$  substitution in lithochlebite–watkinsonite seems likely (Fig. 3). Lithochlebite from Zálesí is a Se-dominant and virtually S-free mineral (S contents of only up to 0.02 *apfu*); similar low sulfur contents were deter-

mined for watkinsonite from Zálesí (Topa *et al.* 2010a, Sejkora *et al.*, in prep.) and Niederschlema–Alberoda (Förster *et al.* 2005). In contrast, Johan *et al.* (1987) reported S contents in the range 1.62–1.82 *apfu* in watkinsonite from the Otish Mountains. The empirical formula of lithochlebite, calculated from average compositions (Table 2) on the basis 15 *apfu*, is  $(\text{Ag}_{1.84}\text{Cu}_{0.03})_{\Sigma 1.87}(\text{Pb}_{1.09}\text{Cd}_{0.01})_{\Sigma 1.10}\text{Bi}_{3.99}\text{Se}_{8.04}$  (Salzburg data) or  $(\text{Ag}_{2.03}\text{Cu}_{0.06})_{\Sigma 2.09}\text{Pb}_{1.01}(\text{Bi}_{3.89}\text{Sb}_{0.05})_{\Sigma 3.94}\text{Se}_{7.96}$  (Brno data), respectively. The ideal formula  $\text{Ag}_2\text{PbBi}_4\text{Se}_8$  requires Ag 11.41, Pb 10.96, Bi 44.22, Se 33.41, total 100.00 wt.%.

#### X-RAY POWDER DIFFRACTION

Hand-picked grains of lithochlebite from Zálesí were used to collect the X-ray powder-diffraction pattern on a PANalytical X'Pert Pro diffractometer operating at 40 kV and 30 mA, equipped with a X'Celerator detector and a secondary graphite monochromator. To minimize background, the powdered sample was placed onto a zero-background silicon sample holder. The powder pattern of lithochlebite (Table 3) was collected in the range from 3 to  $68^\circ 2\theta$  using  $\text{CuK}\alpha$  radiation in Bragg–Brentano geometry, with a step width of  $0.02^\circ$  and a counting time of 30 s per step. Positions and intensities of reflections observed were refined using the Pearson VII profile-shape function with the ZDS of package programs (Ondruš 1995). The diffraction maxima obtained were indexed by comparison with theoretical data calculated by the LAZY PULVERIX program (Yvon

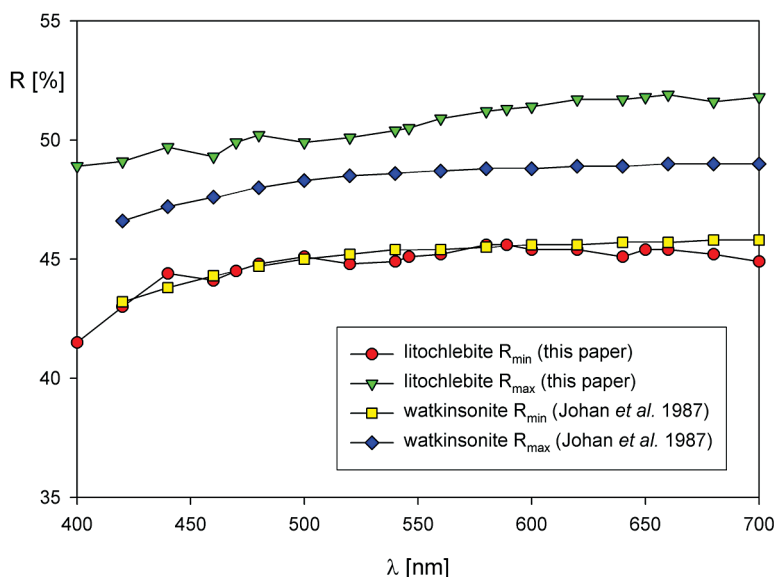


FIG. 2. Reflectance curves in air for a random section of lithochlebite, compared with those of watkinsonite (Johan *et al.* 1987).

TABLE 2. CHEMICAL COMPOSITION OF LITOCHELBITE FROM ZÁLESÍ

	EMP Salzburg (14 anal.)			EMP Brno (19 anal.)			ideal <sup>1</sup>
	mean	std	range	mean	std	range	
Cu wt%	0.10	0.04	0.04 - 0.17	0.21	0.10	0.07 - 0.47	
Ag	10.27	0.76	9.51 - 11.73	11.50	0.44	10.40 - 12.01	11.41
Cd	0.05	0.04	0.00 - 0.14	0.00		0.00 - 0.00	
Pb	11.73	0.18	11.49 - 12.13	10.96	0.24	10.43 - 11.42	10.96
Bi	43.27	0.51	41.93 - 43.70	42.62	0.60	41.23 - 43.38	44.22
Sb	0.00		0.00 - 0.00	0.30	0.07	0.19 - 0.45	
Se	32.93	0.32	32.21 - 33.34	33.01	0.67	31.02 - 34.07	33.41
S	0.01	0.01	0.00 - 0.02	0.01	0.01	0.00 - 0.03	
total	98.36			98.60			100.00
Cu <i>apfu</i>	0.030			0.062			
Ag	1.836			2.030			2.000
Cu+Ag	1.866			2.092			2.000
Cd	0.008			0.000			
Pb	1.092			1.008			1.000
Cd+Pb	1.100			1.008			1.000
Bi	3.991			3.885			4.000
Sb	0.000			0.047			
Bi+Sb	3.991			3.932			4.000
Se	8.039			7.964			8.000
S	0.004			0.004			
Se+S	8.043			7.968			8.000

Atom proportions were calculated on the basis 15 *apfu*; ideal<sup>1</sup>: theoretical composition calculated from the ideal formula  $\text{Ag}_2\text{PbBi}_2\text{Se}_6$ ; std: standard deviations.

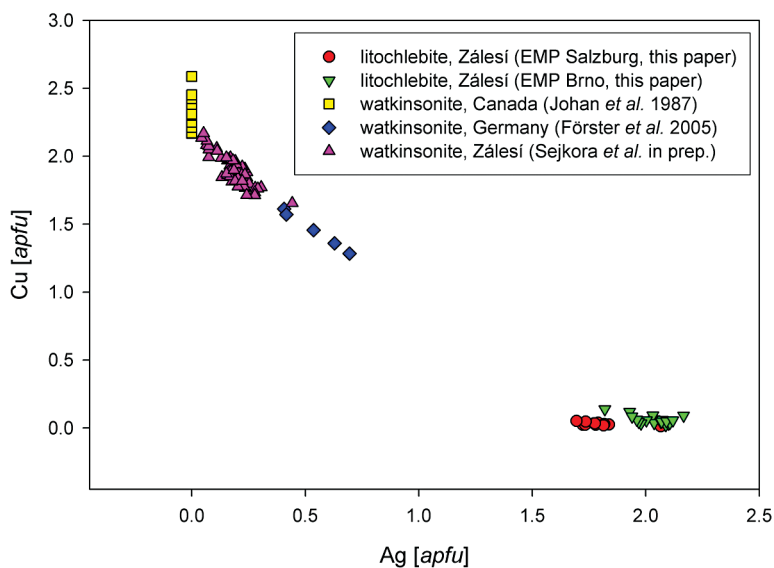


FIG. 3. The plot of Cu and Ag contents for litochlebite and watkinsonite (calculated on the basis of 15 *apfu*).

et al. 1977) from the crystallographic information from the single-crystal study of litochlebite. The unit-cell parameters, refined using the least-squares refinement program of Burnham (1962), are  $a$  13.182(2),  $b$  4.1840(8),  $c$  15.299(2) Å,  $\beta$  109.11(1)°,  $V$  797.3(2) Å<sup>3</sup>,  $a:b:c = 3.1506:1:3.6565$ .

### CRYSTAL-STRUCTURE SOLUTION AND REFINEMENT

For the single-crystal investigation, several grains of litochlebite were extracted from the aggregates in a polished section. They were investigated with a Bruker AXS diffractometer equipped with a CCD area detector, using graphite-monochromated MoK $\alpha$  radiation. An irregular fragment with approximate dimensions 0.02 × 0.04 × 0.07 mm was found to be suitable for structural investigation. Experimental data are listed in Table 4. The SMART (Bruker AXS 1998b) system of programs was used for the unit-cell determination and data collection, SAINT+ (Bruker AXS 1998a) for the calculation of integrated intensities and for empirical absorption-correction based on pseudo  $\Psi$ -scans. We chose the space group  $P2_1/m$  as proposed by the program. It is consistent with the monoclinic symmetry of the lattice and intensity statistics. The structure was solved by direct methods (program SHELXS of Sheldrick 1997a)

TABLE 3. X-RAY POWDER PATTERN OF LITOCHELBITE FROM ZÁLESÍ

$l$	$d_{meas}$	$d_{calc}$	$h$	$k$	$l$	$l$	$d_{meas}$	$d_{calc}$	$h$	$k$	$l$
1	11.457	11.475	1	0	$\bar{1}$	4	2.354	2.356	3	1	$\bar{5}$
2	7.388	7.389	1	0	$\bar{2}$	22	2.288	2.289	3	1	3
4	6.544	6.552	2	0	$\bar{1}$	5	2.196	2.195	6	0	2
4	6.231	6.228	2	0	0	9	2.192	2.190	4	1	2
5	5.142	5.141	2	0	1	21	2.185	2.184	6	0	$\bar{3}$
4	4.821	4.819	0	0	3	29	2.123	2.123	3	1	$\bar{6}$
25	4.610	4.611	2	0	$\bar{3}$	31	2.094	2.092	0	2	0
11	4.392	4.390	3	0	$\bar{1}$	9	2.090	2.088	0	1	6
6	4.253	4.251	3	0	$\bar{2}$	7	2.075	2.076	6	0	0
7	4.154	4.152	3	0	0			2.075	3	0	5
3	4.100	4.101	2	0	2	19	2.060	2.061	3	1	4
1	4.015	4.019	0	1	1	12	2.013	2.012	5	1	$\bar{5}$
22	3.823	3.825	3	0	$\bar{3}$			2.012	4	1	3
		3.822	1	0	$\bar{4}$	6	1.9697	1.9701	1	1	6
53	3.684	3.683	3	0	1	5	1.9376	1.9372	2	1	7
39	3.625	3.621	0	1	2	12	1.9300	1.9304	5	0	7
11	3.616	3.614	0	0	4	11	1.9166	1.9169	6	1	$\bar{1}$
9	3.473	3.473	2	1	0	17	1.9123	1.9130	3	1	7
8	3.334	3.334	1	1	2	14	1.8406	1.8417	6	0	2
10	3.318	3.321	2	0	3	16	1.8180	1.8191	3	2	1
		3.316	3	0	4	2	1.8092	1.8106	0	2	4
76	3.201	3.202	1	0	4	5	1.7853	1.7851	6	0	7
100	3.028	3.029	3	1	$\bar{1}$	4	1.7804	1.7793	5	1	3
88	2.980	2.982	3	1	$\bar{2}$	7	1.7614	1.7624	5	0	$\bar{8}$
95	2.892	2.891	0	0	5	2	1.7514	1.7513	1	2	4
35	2.822	2.823	3	1	$\bar{3}$	9	1.7110	1.7105	1	0	8
23	2.735	2.734	3	0	3	15	1.6959	1.6949	0	2	5
5	2.636	2.636	5	0	2	11	1.6595	1.6580	6	0	8
9	2.632	2.633	1	0	5	10	1.5101	1.5107	6	2	$\bar{3}$
13	2.600	2.599	3	1	$\bar{4}$	6	1.4860	1.4858	6	1	4
17	2.584	2.585	5	0	$\bar{3}$	7	1.4294	1.4305	2	1	$\bar{10}$
11	2.576	2.578	4	1	$\bar{1}$	9	1.4191	1.4191	4	1	7
22	2.453	2.453	2	1	5			1.4187	5	2	7
4	2.380	2.379	0	1	5						

and difference-Fourier syntheses (program SHELXL of Sheldrick 1997b). Refinement data are given in Table 4; fractional coordinates and anisotropic displacement parameters of atoms are listed in Table 5. The principal interatomic distances are presented in Table 6, and selected geometrical parameters for individual coordination polyhedra, calculated with the program IVTON program (Balić-Žunić & Vicković 1996), are given in Table 7. A table of structure factors for litochlebite may be obtained from the Depository of Unpublished Data on the Mineralogical Association of Canada website [document Litochlebite CM49\_639]. Atom labeling is shown in Figure 4, and the crystal structure is illustrated in Figures 5 and 6.

TABLE 4. SINGLE-CRYSTAL X-RAY DIFFRACTION OF LITOCHELBITE: EXPERIMENTAL AND REFINEMENT DETAILS

Crystal data	
Chemical formula	Ag <sub>2</sub> PbBi <sub>3</sub> Se <sub>8</sub>
Chemical formula weight	1890.5
Crystal system	Monoclinic
Space group	$P2_1/m$
Unit-cell parameters	
$a$ , $b$ (Å)	13.203(4), 4.186(1)
$c$ (Å), $\beta$ (°)	15.280(4), 109.164(4)
$V$ (Å <sup>3</sup> )	797.7(4)
$Z$	2
$D_x$ (mg m <sup>-3</sup> )	7.87
No. of reflections for cell parameters	1126
$\mu$ (mm <sup>-1</sup> )	75.1
Crystal form	irregular
Crystal size (mm)	0.05 × 0.07 × 0.10
Crystal color	black
Data collection	
$T_{min}$ , $T_{max}$	0.136, 0.767
No. of measured reflections	3793
No. of independent reflections	938
No. of observed reflections	745 for $F_o > 4\sigma(F_o)$
Criterion for observed reflections	$I > 2\sigma(I)$
$R_{int}$	10.7%
$\theta_{max}$ (°)	20.8
Range of $h$ , $k$ , $l$	$-12 \leq h \leq 13$ , $-4 \leq k \leq 4$ , $-15 \leq l \leq 15$
Refinement	
Refinement on $F_o^2$	
$R_i [F_o > 4\sigma(F_o)]$ (%)	3.89
$wR$ ( $F_o^2$ ) (%)	5.34
$S$ ( $GooF$ )	0.837
No. of reflections used	938
No. of parameters refined	104
Weighting scheme	$w = 1/[\sigma^2(F_o^2) + (0.042 P)^2 + 59.8P] / w = 1/[\sigma^2(F_o^2) + (0.042 P)^2 + 59.8P]$ , where $P = (F_o^2 + 2F_c^2)/3$
$(\Delta\rho)_{max}$	0.000
$\Delta\rho_{max}$ (e/Å <sup>3</sup> )	4.65 [1.61 Å from Ag2a]
$\Delta\rho_{min}$ (e/Å <sup>3</sup> )	-1.81 [1.39 Å from Se5]
Extinction coefficient	0.00005(8)
Source of atomic scattering factors	International Tables for Crystallography Vol. C, Tables 4.2.6.8 and 6.1.1.4)
Computer programs	
Structure solution	SHELXS97 (Sheldrick 1997a)
Structure refinement	SHELXL97 (Sheldrick 1997b)



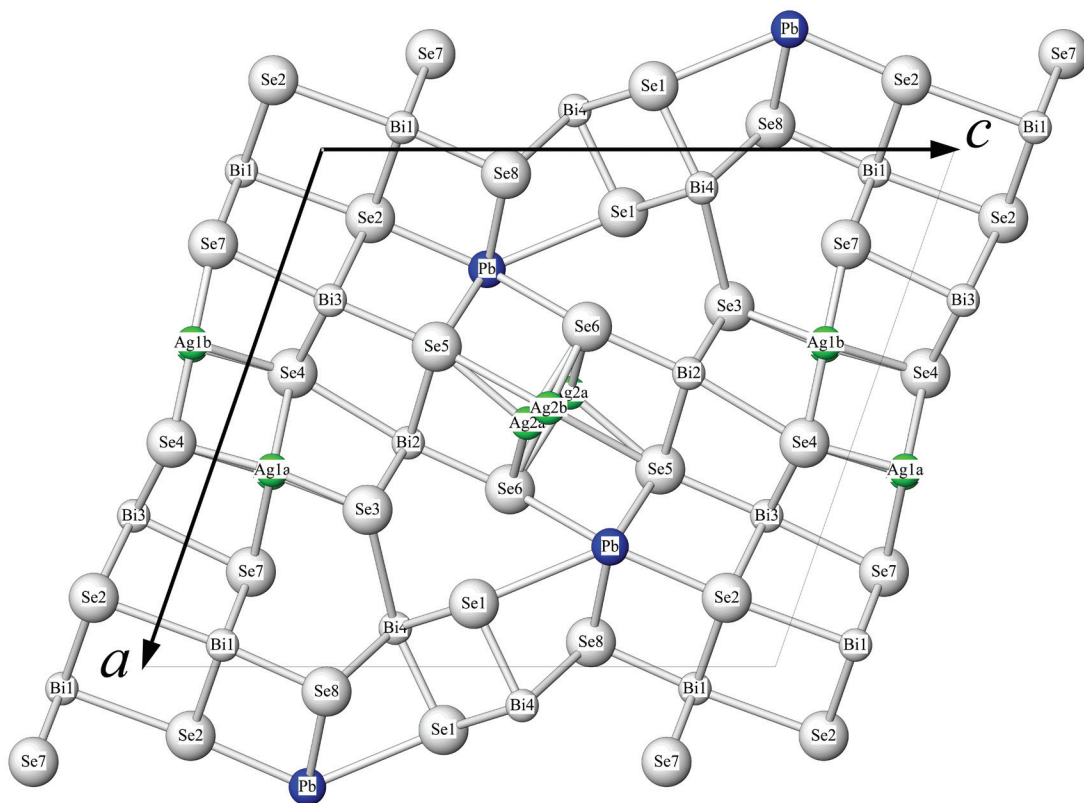


FIG. 4. Atom labeling for the crystal structure of litochlebite. Positions Ag1a and Ag1b as well as Ag2a and Ag2b nearly overlap in this projection upon (010).

TABLE 5. POSITIONAL AND ANISOTROPIC DISPLACEMENT PARAMETERS FOR LITOCHELBITE FROM ZÁLESÍ

ATOM	x	y	z	sof	$U_{eq}$	$U_{11}$	$U_{22}$	$U_{33}$	$U_{13}$
Pb	0.2318(1)	0.25	0.327(1)	1	0.0369(5)	0.0308(9)	0.0238(9)	0.057(1)	0.0161(8)
Bi1	0.0421(1)	0.25	0.8851(1)	1	0.0205(5)	0.0204(8)	0.0215(9)	0.0183(9)	0.0045(6)
Bi2	0.5671(1)	0.25	0.2974(1)	1	0.0201(5)	0.0236(8)	0.0204(9)	0.0176(9)	0.0085(7)
Bi3	0.7082(1)	0.25	0.9039(1)	1	0.0212(5)	0.0217(8)	0.0209(9)	0.0190(9)	0.0040(6)
Bi4	0.9253(1)	0.25	0.3786(1)	1	0.0239(5)	0.0220(8)	0.0218(9)	0.025(1)	0.0031(7)
Se1	0.1219(3)	0.25	0.5106(2)	1	0.0153(9)	0.010(2)	0.018(2)	0.017(3)	0.003(2)
Se2	0.1333(3)	0.25	0.1143(3)	1	0.0174(9)	0.017(2)	0.014(2)	0.021(2)	0.006(2)
Se3	0.3034(3)	0.25	0.7300(3)	1	0.0177(9)	0.019(2)	0.018(2)	0.017(2)	0.007(2)
Se4	0.4329(3)	0.25	0.0765(2)	1	0.0184(9)	0.018(2)	0.018(2)	0.019(2)	0.005(2)
Se5	0.6186(3)	0.25	0.7102(3)	1	0.0194(9)	0.022(2)	0.018(2)	0.019(2)	0.007(2)
Se6	0.6569(3)	0.25	0.4836(3)	1	0.032(1)	0.027(2)	0.057(3)	0.015(2)	0.009(2)
Se7	0.8163(3)	0.25	0.1196(3)	1	0.0204(9)	0.019(2)	0.018(2)	0.023(2)	0.004(2)
Se8	0.9523(3)	0.25	0.6953(2)	1	0.0155(9)	0.017(2)	0.015(2)	0.014(2)	0.005(2)
Ag1a	0.3800(4)	0.25	0.9026(3)	0.86(2)	0.061(3)	0.059(4)	0.11(1)	0.014(3)	0.008(2)
Ag1b	0.374(1)	-0.07(13)	0.902(1)	0.14(2)	0.08(2)	0.01(1)	0.16(5)	0.06(1)	0.004(8)
Ag2a	0.4708(5)	0.25	0.5256(5)	0.76(2)	0.093(4)	0.066(4)	0.125(8)	0.078(5)	0.012(4)
Ag2b	0.5	0	0.5	0.24(2)	0.08(1)				



TABLE 6. SELECTED CATION-ANION DISTANCES (Å) IN LITOCHELBITE FROM ZÁLESÍ

Pb-		Bi1-		Bi2-	
Se5	3.055(3) × 2	Se8	2.749(3)	Se6	2.698(4)
Se2	3.075(3)	Se7	2.823(3) × 2	Se3	2.820(3) × 2
Se8	3.141(3) × 2	Se2	3.123(3) × 2	Se5	3.196(3) × 2
Se6	3.486(4) × 2	Se2	3.309(3)	Se4	3.256(3)
Se1	3.561(4)				
Bi3-		Bi4-		Ag1a-	
Se5	2.803(3)	Se1	2.715(3)	Se3	2.495(6)
Se4	2.882(3) × 2	Se1	2.886(3) × 2	Se4	2.516(5)
Se2	3.037(3) × 2	Se8	3.077(3) × 2	Se4	3.174(5) × 2
Se7	3.133(4)	Se3	3.600(3) × 2	Se7	3.260(5) × 2
		Se7	3.741(5)		
Ag1b-		Ag2a-		Ag2b-	
Se7	2.538(23)	Se6	2.663(5) × 2	Se6	2.407(4) × 2
Se4	2.577(23)	Se6	2.737(9)	Se5	3.250(3) × 2
Se3	2.821(31)	Se5	2.855(7)	Se6	3.815(3) × 2
Se4	2.851(31)	Se5	3.995(7) × 2		
Se3	3.782(43)				
Se4	3.804(43)				

TABLE 7. CHARACTERISTICS OF COORDINATION POLYHEDRA OF CATIONS IN LITOCHELBITE FROM ZÁLESÍ

Atom	1	2	3	4	5	6	7	8
Pb	8	3.226	0.098	0.265	0.920	140.617	58.497	1.912
Bi1	6	3.001	0.119	0.317	0.978	113.219	35.574	3.315
Bi2	6	2.985	0.124	0.327	0.992	111.364	35.292	3.375
Bi3	6	2.964	0.068	0.190	0.997	109.065	34.603	3.267
Bi4	8	3.177	0.191	0.470	0.942	134.265	56.289	3.301
Ag1a	6	2.979	0.016	0.046	0.629	110.737	33.841	1.334
Ag1b	6	2.989	0.254	0.584	0.575	111.840	33.841	1.350
Ag2a	6	3.076	0.264	0.601	0.608	121.878	27.871	1.167
Ag2b	6	3.157	0.000	0.000	0.398	131.833	37.161	1.512

1) coordination number, 2) radius  $r_c$  of a circumscribed sphere, least-squares fitted to the coordination polyhedron, 3) "volume-based" distortion  $u = [V(\text{ideal polyhedron}) - V(\text{real polyhedron})] / V(\text{ideal polyhedron})$ ; the ideal polyhedron has the same number of ligands, 4) "volume-based" eccentricity  $ECC_v = 1 - [(r_c - \Delta)/r_c]^2$ ;  $\Delta$  is the distance between the center of the sphere and the central atom in the polyhedron, 5) "volume-based" sphericity  $SPH_v = 1 - 3\sigma_r$ ;  $\sigma_r$  is a standard deviation of the radius  $r_c$ , 6) volume of the circumscribed sphere, 7) volume of coordination polyhedron, 8) bond-valence sum.

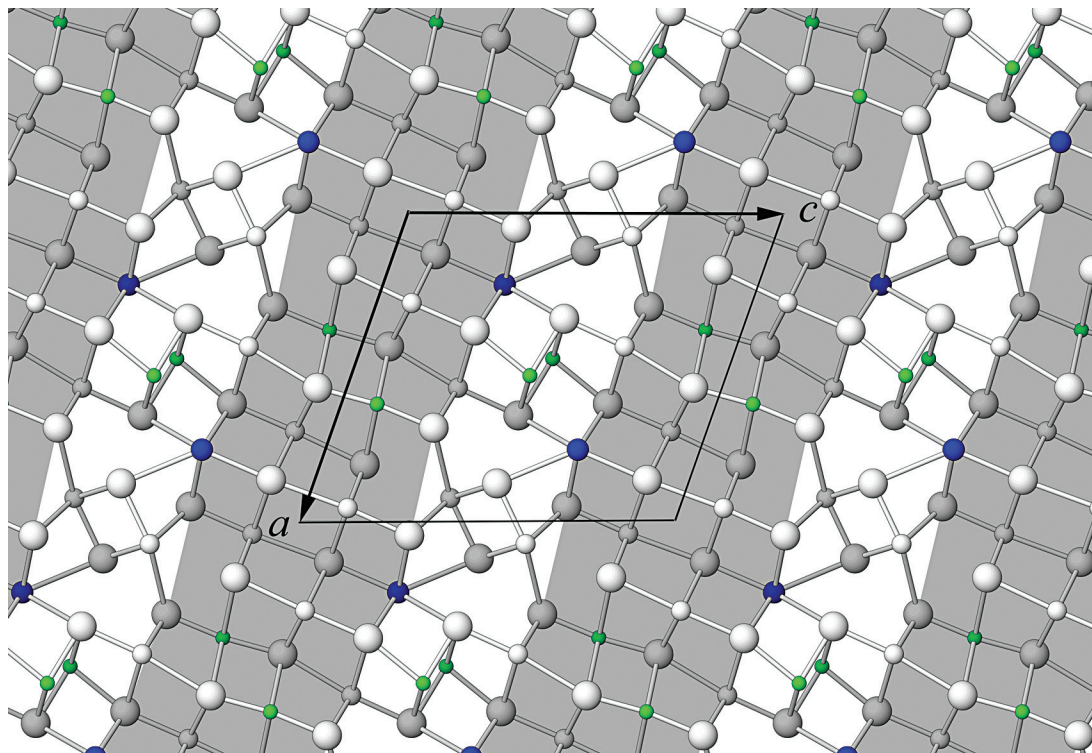


FIG. 5. The crystal structure of lithochelbite in projection on (010). In the order of decreasing size, spheres represent Se, Pb (dark blue), Ag (green, overlaps in the Ag1 and Ag2 sites were simplified), and Bi (white). Shading (white and grey) denotes atoms at two different levels, 2 Å apart). Pseudotetragonal (100) layers that are four atomic levels thick and shaded in the figure alternate with single pseudohexagonal layers of Se atoms that are alternatively coordinated to triangular Ag sites and to bismuth.

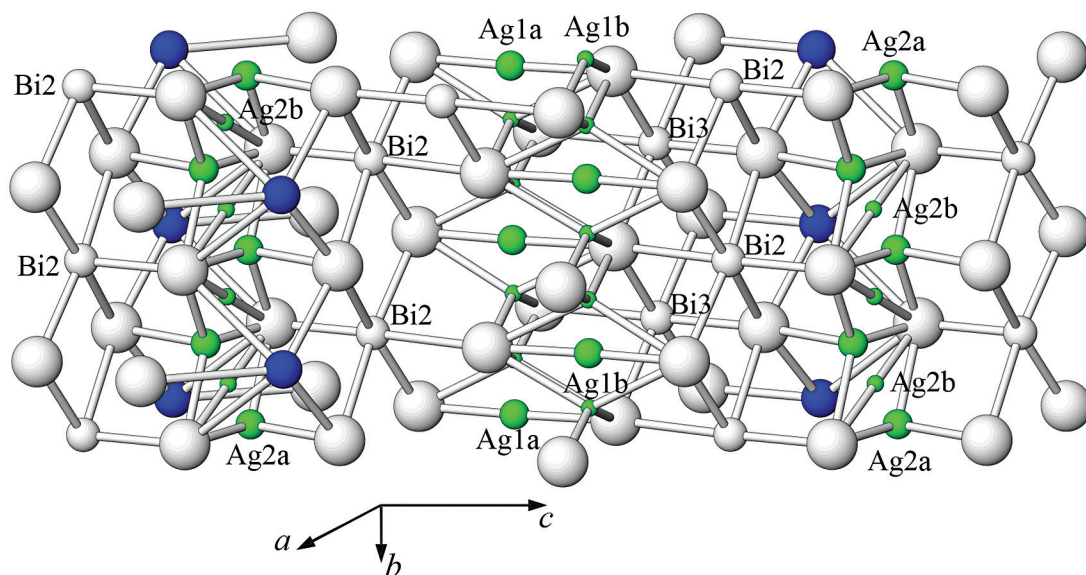


FIG. 6. Coordination of Ag1a, Ag1b, Ag2a and Ag2b in a layer carved out of the structure in the orientation approximately parallel to (001). For conventions, consult Figure 5. Occupancies of silver positions are schematically rendered by the size of the sphere used: small spheres for low occupancies, larger spheres for higher occupancies (detailed information is in Table 5 and discussion in the text).

## DESCRIPTION OF THE STRUCTURE

### General features

Litochlebite and watkinsonite (Topa *et al.* 2010a) are two selenide isotypes broadly related to berryite (Topa *et al.* 2006); the structural description will inevitably concentrate on the similarities and differences observed among phases of this group. As in watkinsonite, the crystal structure of litochlebite contains one Pb site and four distinct Bi sites. Two of the silver sites refined correspond to those of copper sites in watkinsonite; two more are specific to the silver-containing compound.

Similar to isostructural watkinsonite, the crystal structure of litochlebite consists of two alternating types of layers, pseudotetragonal layers that are four atomic sheets thick, and pseudo-hexagonal layers that are formed by a single sheet of anions that contains triangularly coordinated cations (Fig. 5). This figure also shows that the simple picture that ties litochlebite to the remaining phases of this group [watkinsonite (Topa *et al.* 2010a), berryite (Topa *et al.* 2006) and a few synthetic sulfides (Topa *et al.* 2006)] is complicated by the occurrence of paired columns of  $\text{BiS}_5$  coordination pyramids; these protrude into the interspace and draw cations and anions from both the pseudotetragonal surfaces and the pseudo-hexagonal sheet. Although the same occurs in watkinsonite, this phenomenon is much less developed in berryite, where Bi is paired with

Pb, and such a configuration is absent in the synthetic compounds characterized by Topa *et al.* (2006).

### Coordination polyhedra

The Pb and Bi sites have bond-length values (Table 6) very similar to those observed in watkinsonite. The lead coordination polyhedron, in the form of an asymmetric bicapped trigonal prism, recalls such a site in galenobismutite (Pinto *et al.* 2006, Topa *et al.* 2010b). Atoms Bi1–3 are distorted octahedral sites (Table 6), whereas the Bi4 site has square-pyramidal coordination completed to a monocapped trigonal prism (Fig. 4). The largest differences with watkinsonite are observed at the Bi2 site, which is positioned between the Ag1 (litochlebite) or Cu1 (watkinsonite) and Ag2 or Cu2 sites in these structures, and shares edges with them. In the structure of litochlebite, the four bonds situated at the surface of the pseudotetragonal layer are extended (2.820 and 3.196 Å) with respect to those (2.815 and 3.124 Å) in watkinsonite as a direct consequence of the presence of larger Ag1 and Ag2 polyhedra in litochlebite. The apical bond of Bi2 is shorter, being 2.698 Å in litochlebite instead of 2.740 Å in watkinsonite, perhaps as a means of compensation.

The most remarkable feature of the litochlebite structure are the coordination polyhedra of silver (Figs. 4, 6) that “reproduce” faithfully those of copper in watkinsonite. The foreshortened octahedrally coordi-

nated position Ag1a has two opposing short distances, Ag–Se equal to 2.495 and 2.516 Å, respectively, with four long distances equal to 3.174 and 3.260 Å. These values are very similar to the values observed in the foreshortened octahedra in the pseudotetragonal layers of berryite (Topa *et al.* 2006), a *sulfide*, that range from 2.44 to 2.47 Å and from 3.10 to 3.12 Å, respectively. They are longer, however, than the corresponding distances [2.36–2.40 and 3.05–3.17 Å] in the Cu-based foreshortened octahedra in watkinsonite, a *selenide*, with only minor silver contents. The Ag2a site is a distorted tetrahedral site with Ag–Se distances represented by a pair of 2.663 Å bonds and one bond of 2.737 Å in a nearly trigonal planar coordination. The additional bond is 2.855 Å long. The Ag2a site corresponds to the Cu2 site in watkinsonite, with the Cu–Se distances equal to  $2 \times 2.46$ , 2.54, and 2.66 Å, respectively, *i.e.*, the differences in bond lengths are very similar in these two structures.

The Ag1a and Ag2a sites are supplemented in litochlebite by additional partially occupied silver sites. Site Ag1b is a flat tetrahedrally coordinated position flanking the linearly coordinated Ag1a site from both the +c and –c directions, at a distance of only 1.338 Å. The Ag–Se distances in the tetrahedra are 2.538, 2.577, 2.821, and 2.851 Å. The angle of the first two bonds is 145.5°, *i.e.*, it is a bent linear bond. The occupancy of Ag1a has been refined to 0.86 Ag, whereas that of Ag1b to 0.14 Ag. This situation reminds us of the split copper and silver sites in columns of octahedrally coordinated sites in the pavonite homologues (Topa *et al.* 2008).

The column of Ag2a positions is a continuous ribbon of occupied triangles so that the Ag2a–Ag2a distances to the neighbors are 2.447 Å. The refined occupancy is 0.76 Ag. The positions with triangular coordination are separated by linear ones, Ag2b, with occupancy 0.24 Ag, situated on the inclined sides of these triangles. The Ag2a–Ag2b distance is only 1.22 Å, *i.e.*, they cannot both be occupied. The linear coordination is  $2 \times 2.406$  Å; the next nearest Se atoms are at 3.203 Å, and the nearest Ag2b sites are at only 2.093 Å. This situation suggests that at least the Ag2 sites represent a frozen or a partly frozen array of silver atoms that were mobile along the [010] channels at the conditions of formation. Partial mobility is also suggested by the  $U_{22}$  components of the anisotropic displacement (Table 5). The quality of the diffraction data ( $R_{\text{int}} = 10.7\%$ ), caused by the quality of the material available (Fig. 1), does not warrant a refinement of the structure with anharmonic displacement parameters.

#### *Comparison with the structures of watkinsonite and berryite*

Topa *et al.* (2010a) suggested that the Cu2 configuration in watkinsonite, and the occurrence of vacant triangular sites in its pseudohexagonal layers, are a

consequence of the replacement of the foreshortened Ag1a octahedron in the pseudotetragonal layer of berryite by a smaller Cu1 octahedron in watkinsonite. This might seem to contradict the cases of the present structure, in which the site with octahedral coordination is occupied by silver. However, the tetrahedrally coordinated site (Ag2a here) is occupied by *silver* and not by copper as in berryite. As a consequence, it is larger, so that the size ratio between the octahedra and the tetrahedra (both Ag) in litochlebite is the same as that in watkinsonite (in which both positions are occupied by copper). Thus, the size ratio does not correspond to that in berryite, with Ag–S octahedra and Cu–S tetrahedra. In both litochlebite and watkinsonite, the presence of Bi4 instead of Pb, as was seen in every second pseudotetragonal slab in berryite, contributes to the creation of  $M^+$  vacancies in the pseudohexagonal layer.

Litochlebite has a unit-cell volume 3.3% larger than the isostructural watkinsonite, although 9% Cu in the latter is replaced by Ag (Table 8). It contains Ag in the Ag1 positions, like berryite, but the pseudotetragonal layers have protruding Bi4 atoms on both surfaces, like in watkinsonite, and not combinations of slabs with either Pb or Bi on the opposite surfaces, as in the monoclinic berryite. Thus, the *c* parameter and  $d_{001}$  are not doubled as in berryite. Therefore,  $c_{\text{lit}}$  is equal to 15.299 Å, whereas  $c_{\text{ber}}$  is 28.925 Å, with the  $\beta$  angle of berryite smaller than that of litochlebite (Topa *et al.* 2006). Although it has a closely related structure, litochlebite is not a polytype of berryite.

#### RELATIONS TO OTHER SULFOSALTS

As already mentioned, litochlebite is an Ag-dominant and S-free analogue of watkinsonite  $\text{Cu}_2\text{PbBi}_4\text{Se}_8$  (Johan *et al.* 1987, Förster *et al.* 2005, Topa *et al.* 2010a, Sejkora *et al.*, in prep.) and is structurally related to berryite (Topa *et al.* 2006, compare Figs. 4 and 6 in Topa *et al.* 2010a). Together, these three structures represent a remarkable case of silver and copper replacing one another in several structural roles, a case that is less frequent than commonly believed. The comparison of litochlebite with watkinsonite is given in the Table 8 and Figure 3. Together with berryite and watkinsonite, litochlebite differs substantially from the sulfosalts of the proudite–felbertalite and junoite groups. Members of these groups have composite layer structures modified by periodic steps that accommodate copper sites. As a consequence, both the pseudotetragonal and the pseudohexagonal layers in them are divided into finite-size fragments that are joined *en échelon*, with small layer overlaps in the case of pseudohexagonal layers. Fragmentation, steps and overlaps do not occur in the structures of the berryite–litochlebite group.

Besides the obvious modular affinity of these sulfosalts to cannizzarite, an archetypal composite layer structure consisting of unmodified alternating pseudo-

TABLE 8. COMPARISON OF LITOCHELBITE AND WATKINSONITE

	litochlebite Zálesí, Czech Republic this paper	watkinsonite* Zálesí, Czech Republic Topa <i>et al.</i> (2010a)	watkinsonite Otish Mountains, Canada Johan <i>et al.</i> (1987)	watkinsonite Niederschlema – Alberoda, Germany Förster <i>et al.</i> (2005)
ideal formula	Ag <sub>2</sub> PbBi <sub>4</sub> Se <sub>8</sub>	Cu <sub>2</sub> PbBi <sub>4</sub> Se <sub>8</sub>	Cu <sub>2</sub> PbBi <sub>4</sub> (Se,S) <sub>8</sub>	(Cu,Ag) <sub>2</sub> PbBi <sub>4</sub> Se <sub>8</sub>
Ag + Cu sites	Ag <sub>1.84</sub> Cu <sub>0.03</sub>	Cu <sub>1.90</sub> Ag <sub>0.19</sub>	Cu <sub>2.30</sub>	Cu <sub>1.46</sub> Ag <sub>0.54</sub>
Se + S sites	Se <sub>8.04</sub>	Se <sub>7.88</sub> S <sub>0.05</sub>	Se <sub>8.07</sub> S <sub>1.71</sub> Te <sub>0.04</sub>	Se <sub>7.99</sub> S <sub>0.04</sub>
crystal system	monoclinic	monoclinic	monoclinic	-
space group	<i>P2<sub>1</sub>/m</i>	<i>P2<sub>1</sub>/m</i>	<i>P2<sub>1</sub>/m, P2</i> or <i>Pm</i>	-
<i>a</i> [Å]	13.182(2)	12.952(4)	12.921(3)	-
<i>b</i> [Å]	4.1840(8)	4.152(1)	3.997(1)	-
<i>c</i> [Å]	15.299(2)	15.155(5)	14.989(3)	-
β [°]	109.11(1)	108.931(5)	109.2(2)	-
<i>V</i> [Å <sup>3</sup> ]	797.3(2)	770.9(8)	731	-
<i>Z</i>	2	2	2	-
<i>d</i> (301)	3.684(53)	3.629(23)	3.573(90)	-
<i>d</i> (104)	3.201(76)	3.173(30)	3.133(50)	-
<i>d</i> (31 $\bar{1}$ )	3.028(100)	2.992(100)	2.976(100)	-
<i>d</i> (31 $\bar{2}$ )	2.980(88)	2.946(70)	2.929(100)	-
<i>d</i> (005)	2.892(95)	2.867(40)	2.831(50)	-

\* The data for watkinsonite from Zálesí are based on single-crystal investigations.

tetragonal and pseudo-hexagonal layers, litochlebite, watkinsonite and berryite are also related to the pavonite homologous series in a way described and illustrated by Topa *et al.* (2006, 2010a). In the case of litochlebite, fully analogous to that of watkinsonite (Fig. 4 in Topa *et al.* 2010a), the pavonite-like portions of the structure are wavy (10 $\bar{1}$ ) slabs which include Ag1, Bi2, and Bi4 sites, with Bi3 sites on slab boundaries. They are separated by intervening slabs of lesser thickness, based on the Pb and Ag<sub>2</sub> sites.

#### ACKNOWLEDGEMENTS

The authors thank to Radek Škoda (Masaryk University, Brno) and Zdeněk Němec (Havířov) for their kind support of this study. This work was financially supported by Ministry of Culture of the Czech Republic (DE07P04OMG003) and by grant no. 272–08–0227 of the Research Council for Nature and Universe (Denmark) as well as by Christian Doppler Stiftung (Austria). Thorough reviews by H.-J. Förster and an anonymous reviewer, as well as the editorial care of Robert F. Martin, are gratefully acknowledged.

#### REFERENCES

- BALIĆ-ŽUNIĆ, T. & VICKOVIĆ, I. (1996): IVTON – program for the calculation of geometrical aspects of crystal structures and some crystal chemical applications. *J. Appl. Crystallogr.* **29**, 305–306.
- BRUKER AXS (1998a): SAINT, Version 5.0. Bruker AXS, Inc., Madison, Wisconsin 53719, USA.
- BRUKER AXS (1998b): SMART, Version 5.0. Bruker AXS, Inc., Madison, Wisconsin 53719, USA.
- BURNHAM, C.W. (1962): Lattice constant refinement. *Carnegie Inst. Wash., Yearbook* **61**, 132–135.
- DOLNÍČEK, Z., FOJT, B., PROCHASKA, W., KUČERA, J. & SULOVSÝ, P. (2009): Origin of the Zálesí U–Ni–Co–As–Ag/Bi deposit, Bohemian Massif, Czech Republic: fluid inclusion and stable isotopes constraints. *Mineral. Deposita* **44**, 81–97.
- FOJT, B., DOLNÍČEK, Z., KOPA, D., SULOVSÝ, P. & ŠKODA, R. (2005): Paragenesis of hypogene associations from the uranium deposit at Zálesí near Rychlebské hory Mts., Czech Republic. *Čas. Slez. Muž. Oprava (A)* **54**, 223–280 (in Czech).
- FÖRSTER, H.-J., TISCHENDORF, G. & RHEDE, D. (2005): Mineralogy of the Niederschlema–Alberoda U–Se–polymetallic deposit, Erzgebirge, Germany. V. Watkinsonite, nevskite, bohdanowiczite and other bismuth minerals. *Can. Mineral.* **43**, 899–908.
- FROST, R.L., BAHFENNE, S., ČEJKA, J., SEJKORA, J., PLÁŠIL, J. & PALMER S.J. (2010a): Raman spectroscopic study of the hydrogen-arsenate mineral pharmacolite Ca(AsO<sub>3</sub>OH)•2H<sub>2</sub>O – implication for aquifer and sediment remediation. *J. Raman Spectrosc.* **41**, 1348–1352.
- FROST, R.L., REDDY, B.J., SEJKORA, J., ČEJKA, J. & KEEFFE, E.C. (2010b): Characterisation of the copper arsenate min-



- eral strashimirite,  $\text{Cu}_8(\text{AsO}_4)_4(\text{OH})_4 \cdot 4\text{H}_2\text{O}$ , by near infrared spectroscopy. *J. Near Infrared Spectrosc.* **18**, 157-165.
- FROST, R.L., SEJKORA, J., ČEJKA, J. & KEEFFE, E.C. (2009): Vibrational spectroscopic study of the arsenate mineral strashimirite  $\text{Cu}_8(\text{AsO}_4)_4(\text{OH})_4 \cdot 5\text{H}_2\text{O}$  – relationship to other basic copper arsenates. *Vibrat. Spectrosc.* **50**, 289-297.
- JOHAN, Z., PICOT, P. & RUHLMANN, F. (1987): The ore mineralogy of the Otish Mountains uranium deposit, Quebec: skippenite,  $\text{Bi}_2\text{Se}_2\text{Te}$ , and watkinsonite,  $\text{Cu}_2\text{PbBi}_4(\text{Se,S})_8$ , two new mineral species. *Can. Mineral.* **25**, 625-638.
- ONDRUŠ, P. (1995): ZDS – software for analysis of X-ray powder diffraction patterns. Version 6.01. User's guide. Praha, Czech Republic.
- PINTO, D., BALIĆ-ŽUNIĆ, T., GARAVELLI, A., MAKOVICKY, E. & VURRO, F. (2006): Comparative crystal-structure study of Ag-free lillianite and galenobismutite from Vulcano, Aeolian Islands, Italy. *Can. Mineral.* **44**, 159-175.
- POUCHOU, J.L. & PICOIR, F. (1985): "PAP"  $\phi(\rho Z)$  procedure for improved quantitative microanalysis. In *Microbeam Analysis* (J. T. Armstrong, ed.). San Francisco Press, San Francisco, California (104-106).
- SEJKORA, J., PAULIŠ, P. & MALEC, J. (2004): Supergene selenium mineralization at the uranium deposit Zálesí, Rychlebské hory Mountains. *Bull. mineral.-petrol. odd. Nár. Muz. (Praha)* **12**, 174-179 (in Czech).
- SEJKORA, J., PAULIŠ, P. & TVRDÝ, J. (2008): Zálesí – eine interessante Mineralfundstelle an der tschechisch-polnischen Grenze. *Lapis* **33**, 22-36.
- SEJKORA, J., ŘÍDKOŠIL, T. & ŠREIN, V. (1999): Zálesíite, a new mineral of the mixite group, from Zálesí, Rychlebské Hory Mts., Czech Republic. *Neues Jahrb. Mineral., Abh.* **175**, 105-124.
- SEJKORA, J., ŠKODA, R. & PAULIŠ, P. (2006): Selenium mineralization of the uranium deposit Zálesí, the Rychlebské Hory Mts., Czech Republic. *Mineral. Polonica, Spec. Pap.* **28**, 196-198.
- SHELDRIK, G.M. (1997a): *SHELXS-97. A Computer Program for Crystal Structure Determination*. University of Göttingen, Göttingen, Germany.
- SHELDRIK, G.M. (1997b): *SHELXL-97. A Computer Program for Crystal Structure Refinement*. University of Göttingen, Göttingen, Germany.
- TOPA, D., MAKOVICKY, E., PUTZ, H. & MUMME, W.G. (2006): The crystal structure of berryite,  $\text{Cu}_3\text{Ag}_2\text{Pb}_3\text{Bi}_7\text{S}_{16}$ . *Can. Mineral.* **44**, 465-480.
- TOPA, D., MAKOVICKY, E. & BALIĆ-ŽUNIĆ, T. (2008): What is the reason of the doubled unit-cell volumes of copper-lead-rich pavonite homologues? The crystal structures of cupromakovickyite and makovickyite. *Can. Mineral.* **46**, 515-523.
- TOPA, D., MAKOVICKY, E. & PUTZ, H. (2010b): The crystal structure of angelaite,  $\text{Cu}_2\text{AgPbBiS}_4$ . *Can. Mineral.* **48**, 145-153.
- TOPA, D., MAKOVICKY, E., SEJKORA, J. & DITTRICH, H. (2010a): The crystal structure of watkinsonite,  $\text{Cu}_2\text{PbBi}_4\text{Se}_8$ , from the Zálesí uranium deposit, Czech Republic. *Can. Mineral.* **48**, 1109-1118.
- YVON, K., JEITSCHKO, W. & PARTHÉ, E. (1977): LAZY PULVERIX, a computer program, for calculation X-ray and neutron diffraction powder patterns. *J. Appl. Crystallogr.* **10**, 73-74.

Received July 12, 2010, revised manuscript accepted March 1, 2011.